Available online at www.sciencedirect.com

ScienceDirect

Procedia CIRP 41 (2016) 1055 – 1060

www.elsevier.com/locate/procedia

48th CIRP Conference on MANUFACTURING SYSTEMS - CIRP CMS 2015

Advanced ultrasonic non-destructive evaluation for metrological analysis and quality assessment of impact damaged non-crimp fabric composites

Tiziana Segreto*, Alberto Bottillo, Roberto Teti

Fraunhofer Joint Laboratory of Excellence on Advanced Production Technology (Fh-J_LEAPT Naples)
Dept. of Chemical, Materials and Industrial Production Engineering, University of Naples Federico II, Piazzale Tecchio 80, Naples 80125, Italy

* Corresponding author. Tel.: +393471337695; fax: +390817682362. E-mail address: tsegreto@unina.it

Abstract

Composite materials are nowadays massively utilized in a very large number of industrial applications. Thus, it has become essential to characterize the service behaviour they can provide depending on their working conditions. In this paper, the study of the influence of impact conditions on damage generation in high performance composite materials, consisting of non-crimp fabric composite laminates, is carried out through the application of an advanced ultrasonic non-destructive evaluation technique, known as full volume ultrasonic scanning. This technique is based on the pulse-echo immersion testing method and allows for the quantitative analysis of the internal material structure in the entire composite volume. The aim of the ultrasonic non-destructive evaluation analysis is the metrological characterization of the non-crimp fabric composite laminates in terms of actual thickness estimation and stacking sequence fiber orientation verification as well as their quality assessment in terms of impact damage development within the whole composite material volume.

Keywords: Non-crimp fabric composite materials; Impact testing; Ultrasonic non-destructive evaluation; Damage assessment

1. Introduction

The employment of carbon fiber reinforced plastic (CFRP) composites is steadily increasing in diverse manufacturing sectors such as in the automotive industry for chassis and structural parts in high performance vehicles; in the renewable energy industry for wind turbine blades; and in the aerospace industry to achieve lighter airframe structures [1]. Today, the main aircraft companies, Airbus and Boeing, utilize composites for their airplane construction to reduce fuel consumption, engine emissions and operating costs [2].

CFRP composites are successfully used whenever high strength to-weight-ratio, high stiffness to-weight-ratio and high rigidity are required. Despite these advantages, one of the main drawbacks of these advanced materials is still their high cost due to the raw materials, manufacturing complexity, and expensive processing equipment.

The utilization of non-crimp fabric (NCF) composite materials as alternatives to prepreg composites reduces material related costs and high energy impacts due to expensive prepregging operations. NFC composites are made of several layers stitched together by a stitching yarn. The benefit of NCF composites is that their fibers are not crimped and one macroscopic layer, which consists of different sub-layers, can be processed instead of several sub-layers [3].

Despite the lack of crimp in NCF composites, their mechanical properties are lower than those of the equivalent unidirectional laminates [4-6]. The cause is the existence of some waviness in the material structure due to stitching, particularly in the fabric plane rather than through the thickness, as is the case with woven composite materials. Hence, the effect of stitching on the mechanical performance and damage development of NCF composites needs to be carefully evaluated.

The effect of damage, given by stiffness-damage relationships, has been a subject of extensive research for laminated composites in recent years [7-9].

doi:10.1016/j.procir.2015.12.125

Damage evaluation after impact load is useful to determine the NCF composite residual properties. The interaction between failure modes is also critical to understand damage mode initiation and propagation in these new materials [10].

As it has been found that even low impact energy can determine relevant strength losses in composites, extensive efforts have been devoted to study the relationships between impact parameters, failure modes, damage extension and residual strength retention after impact [11].

In this paper, an advanced ultrasonic (UT) non-destructive (NDE) technique [12], known as full volume (FV) UT scanning [13], was applied to quadriaxial NCF composites under impact damage conditions.

The goal of the UT NDE analysis is the metrological assessment of the NCF composites, including actual thickness estimation and correct stacking sequence verification, as well as the characterization of impact damage development within the entire composite material volume, comprising the identification of damage position in the thickness direction and damage transition in the laminate stacking sequence.

2. Materials and impact testing

2.1 Materials

The carbon fiber reinforced plastic (CFRP) composites under examination are 4 mm thick non-crimp fabric (NCF) laminates manufactured using resin infusion under flexible tooling (RIFT) technology [14]. In the RIFT process, reinforcing fibers are first placed on a female mould and then a flexible tooling coating is placed over the fibers and sealed around the edges in vacuum tight manner. The resin is drawn in the mould by vacuum action and impregnates the preform. The shape of the part is obtained by vacuum infusion of the fibers between mould and flexible tooling coating [15].

Quadriaxial laminates were manufactured with the following symmetrical stacking sequence: $[+45°/0°/-45°/90°, +45°/0°/-45°/90°, 90°/-45°/0°/+45°, 90°/-45°/0°/+45°]_s$. The plastic matrix was Hexcel HexPly®M36 epoxy resin and the carbon fibers type was Tenax HTS 5632 12k. Polyester stitching yarn (50 dtex) was used for joining with 2.5 mm stitch length. Final fiber aerial weight per single orientation layer was 267 g/m^2 and final fiber volume fraction was 62%.

Rectangular specimens of 100 mm x 150 mm size were cut from the manufactured laminates (Fig. 1).

2.2 Impact testing

Dynamic impact testing was performed on a CEAST Fractovis MK4 falling weight machine using a cylindrical indenter with hemispherical nose. NCF composite rectangular specimens were clamped in an appropriate fixture. The Das 4000 dedicated software was used for impact test data recording. Diverse impact energies were employed for the testing campaign: 9, 12, 16, 20, 25, 30, 40 J. In Table 1, the selected parameters for the impact testing plan are reported.

3. Ultrasonic non-destructive evaluation

A pulse-echo immersion ultrasonic (UT) testing technique [12] was applied for non-destructive evaluation (NDE) of the NCF composites. Full volume (FV) UT scanning [13], based on complete UT waveform acquisition allowing for UT computerized axial tomography, was utilized to quantitatively analyze the internal material structure of the entire NCF composite volume. The used UT NDE system is made of a purposely designed hardware configuration and a custom made software code, RoboTest© v.2.0, developed in LabView© at the Fraunhofer Joint Laboratory of Excellence on Advanced Production Technology, Naples, Italy [16].

3.1. UT NDE system hardware configuration

The advanced UT NDE system hardware configuration is schematically shown in Fig. 2 and consists of:

- Oscillator/detector, generating electrical pulses for UT probe excitation and receiving the returning UT signals
- Transmitter/receiver high frequency focused UT immersion probe with high damping characteristics for pulse-echo testing
- Digital oscilloscope connected to the oscillator/detector for visualisation and digitisation of UT signals
- PC for UT waveform acquisition from the digital oscilloscope through GPIB interface, UT signal storage for post-processing and UT probe displacement control
- Mechanical UT probe displacement system, made up of a 6-axis Staubli RX 60 L robotic arm

(a)

(b)

Fig.1. NCF composite laminates manufactured by RIFT technology: (a) not impacted sample QHL3IM1, (b) impacted sample QHL3IM2.

Table 1. Parameters of the impact testing plan.

Sample ID	Height (m)	Mass (kg)	Impact energy (J)	Speed (m/s)
QHL3IM1	-	-	-	-
QHL3IM2	0.255	3.6	9	2.24
QHL3IM3	0.340	3.6	12	2.58
QHL3IM4	0.453	3.6	16	2.98
QHL3IM5	0.567	3.6	20	3.33
QHL3IM6	0.708	3.6	25	3.73
QHL3IM7	0.546	5.6	30	3.27
QHL3IM8	0.728	5.6	40	3.78

3.2. UT NDE custom made software code

RoboTest© v.2.0 is a custom made software code, developed in LabView© at the Fraunhofer Joint Laboratory of Excellence on Advanced Production Technology, Naples, Italy [16], capable to control the displacement of the UT NDE robotic system with 6 degrees of freedom and provide for UT waveform signal detection, storage and analysis. It contains various test mode options: here, the full volume ultrasonic (FV-UT) scan procedure, based on pulse-echo immersion testing, was used (Fig. 3). It entails detecting and digitizing the entire UT waveform for each probe position during x-y raster scanning of NCF laminates. The UT data are stored in a volumetric file containing the whole set of digitized UT waveforms for each material interrogation point.

3.3. UT NDE through FV-UT scanning

Pulse-echo immersion FV-UT scans were executed with:

- Focused (49.6 mm focal length) high frequency (15 MHz) highly damped immersion UT probe
- Oscillator/detector set at 90 dB gain & medium damping
- Digital oscilloscope set at 1 V (Volts/div), 0.5 μs (Time/div) and 100 MHz sampling frequency, resulting in 500 samplings for each detected UT waveform
- For all NCF specimens, scanning area was 110 mm x 155 mm and boustrophedonic raster scan step was 1 mm

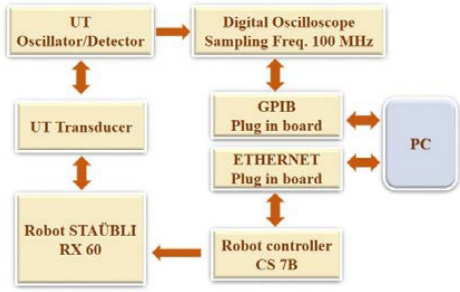

Fig. 2. Ultrasonic NDE system.

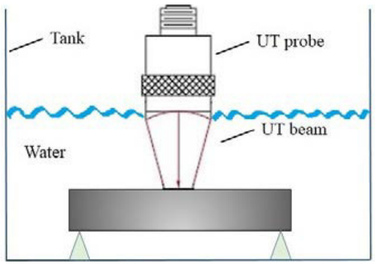

Fig. 3. Pulse-echo UT immersion testing with focused UT probe.

4. Ultrasonic image generation

From the acquired UT volumetric file, containing all the waveforms stored during FV-UT scanning, single or multiple UT images of any thickness portion of the internal structure of the NCF composite under examination can be obtained for analysis, allowing for UT computerized axial tomography.

To obtain the UT images, it is first necessary to select and retrieve a typical UT waveform from the volumetric file. Then, a time gate is set on this waveform to identify the thickness portion to be imaged. The time gate can be divided into a number of equal sub-gates to obtain multiple images of the selected thickness portions. As the time axis orientation corresponds to the UT propagation in the NCF composite thickness direction, the sub-gate width identifies the thickness portion to be imaged. One image is generated for each sub-gate and each image represents the internal structure of the corresponding thickness portion of the NCF composite.

5. UT nondestructive evaluation of NCF composites

5.1. Metrological characterization

The metrological characterization of the NCF composite was carried out on the not impacted specimen QHL3IM1 (Fig.1) with the aim to verify the stacking sequence fiber orientations and evaluate the actual laminate thickness.

Fig. 4 reports the typical UT waveform from the QHL3IM1 UT volumetric file. To verify the consistency of fiber orientations with the designed stacking sequence, 16 multiple UT images were generated by setting a time gate on the entire UT waveform and dividing it into 16 sub-gates.

Fig. 5 shows the 16 UT images obtained in this way, whereby each image corresponds to 1/16 of the NCF composite nominal thickness, i.e. 0.25 mm, comprising two diverse consecutive fiber orientations in the stacking sequence (see also Table 2).

The UT waveform enters the NCF laminate after travelling in water and, thus, the initial four images in the top row of Fig. 5 are generated by the UT echo reflected by stacking sequence [+45°/0°/-45°/90°, +45°/0°/-45°/90°] in the first 1 mm thickness portion. Stacking sequence [90°/-45°/0°/+45°, 90°/-45°/0°/+45°] characterizes the second row of four images in Fig. 5, corresponding to the second 1 mm thickness portion. Due to the symmetrical structure of the NCF laminate, the stacking sequence of the third 1 mm thickness portions is [+45°/0°/-45°/90°, +45°/0°/-45°/90°] (third row of four images in Fig. 5) and the stacking sequence of the fourth 1 mm thickness portion is [90°/-45°/0°/+45°, 90°/-45°/0°/+45°] (fourth row of four images in Fig. 5).

The actual thickness s of the not impacted NCF composite specimen QHL3IM1 was estimated through formula:

$$v = \frac{s}{\Delta T / 2} \quad (1)$$

where v is the UT velocity in the NCF composite and ΔT is the time-of-flight (ToF), i.e. the time it takes the UT signal to traverse to and fro the complete NCF composite thickness.

The total time distance measured between the UT front echo and back echo is $\Delta T = 2.665$ μs. By selecting an average UT velocity in the NCF composite equal to 3000 m/s, the thickness of the NCF specimen given by eq. (1) is s = 3.98 mm, which is very close to the nominal thickness of 4 mm.

Table 2. Estimation results for NCF composite thickness portions comprising two diverse consecutive fiber orientations in the laminate stacking sequence.

Stacking sequence thickness portion	**ToFmin [s]**	**ToFmax [s]**	**ΔT = ToFmax –ToFmin [s]**	**Average UT velocity [m/s]**	**Estimated thickness [mm]**
+45°/0°	1.63E-08	1.80E-07	1.64E-07	3000	0.25
-45°/90°	1.80E-07	3.43E-07	1.63E-07	3000	0.24
+45°/0°	3.43E-07	5.07E-07	1.64E-07	3000	0.25
-45/90°	5.07E-07	6.76E-07	1.69E-07	3000	0.25
90°/-45°	6.76E-07	8.45E-07	1.69E-07	3000	0.25
0°/+45°	8.45E-07	1.01E-06	1.65E-07	3000	0.25
90°/-45°	1.01E-06	1.18E-06	1.70E-07	3000	0.26
0°/+45°	1.18E-06	1.34E-06	1.60E-07	3000	0.24
+45°/0°	1.34E-06	1.50E-06	1.60E-07	3000	0.24
-45°/90°	1.50E-06	1.67E-06	1.70E-07	3000	0.26
+45°/0°	1.67E-06	1.84E-06	1.70E-07	3000	0.26
-45°/90°	1.84E-06	2.01E-06	1.70E-07	3000	0.26
90°/-45°	2.01E-06	2.18E-06	1.70E-07	3000	0.26
0°/+45°	2.18E-06	2.34E-06	1.60E-07	3000	0.24
90°/-45°	2.34E-06	2.51E-06	1.70E-07	3000	0.26
0°/+45°	2.51E-06	2.67E-06	1.60E-07	3000	0.24
NCF total thickness	1.07E-08	2.66E-06	2.67E-06	3000	**3.98**

Table 2 reports the thickness estimation of each nominal 0.25 mm portion of the symmetrical NCF stacking sequence [+45°/0°/-45°/90°, +45°/0°/-45°/90°, 90°/-45°/0°/+45°, 90°/-45°/0°/+45°]$_s$. From the table, it can be seen that the estimated thickness portions are all very close to the nominal value of 0.25 mm. The small difference of ±0.01 mm can be attributed to minor variations of the local UT velocity with respect to the selected value of 3000 m/s that represents the average UT velocity in the whole composite volume.

5.2. Impact damage characterization

The characterization of impact damage development within the entire NCF composite volume focused on the damage transition in the laminate stacking sequence and the damage position in the thickness direction. Figs. 6, 7 and 8 show four UT images each, obtained from the UT volumetric files of quadriaxial laminates QHL3IM2, QHL3IM5 and QHL3IM8 impacted with energy 9 J, 20 J and 40 J, respectively. In every figure, each of the four images represents the internal structure of 1/4 of the NCF laminate thickness, i.e. 1 mm, starting from the upper surface (first image on the left) down to the opposite lower surface (last image on the right).

By examining the UT images in the figures, it can be noted that the impact damage develops differently at interfaces between layers with diverse fiber orientations. Moreover, the delamination extension increases with rising distance (depth) from the impact surface and with growing impact energy. This results in the well known hat-shaped configuration of the delamination [17]. The UT analysis also reveals the absence of delamination in a small zone directly below the impact surface contact point.

Figs. 6d, 7d and 8d display UT images that stand for the in-plane projection of the damage developed at different depths in the whole laminate thickness, rather than just the damage in the fourth (lowest) 1 mm thickness portion. Their examination allows to assess the overall damage in the material according to the conventional UT C-scan technique and can be used for total delaminated area measurement.

The damage position in the thickness direction was evaluated by analyzing the 16 UT images generated for every impacted NCF specimen according to the procedure described in section 5.1 (see Fig. 5).

After identifying the image containing the damage and the corresponding laminate thickness portion, the damage position in the thickness direction was evaluated by substituting in eq. (1) the ToF value related to the time gate for that thickness portion.

In Table 3, the damage position is reported for each impacted specimen in terms of start of damage, start of delamination and maximum delamination extension, evaluated from the front surface in the thickness direction.

Table 3. Damage position in the thickness direction and maximum delamination area extension for each impacted sample.

Sample ID	Start of damage [mm]	Start of delamination [mm]	Max delamination extension position [mm]
QHL3IM2	0.311	1.125	2.615
QHL3IM3	0.012	1.125	2.810
QHL3IM4	0.188	1.126	2.555
QHL3IM5	0.062	1.125	2.435
QHL3IM6	0.250	1.125	2.750
QHL3IM7	0.062	1.062	2.510
QHL3IM8	0.006	1.188	2.690

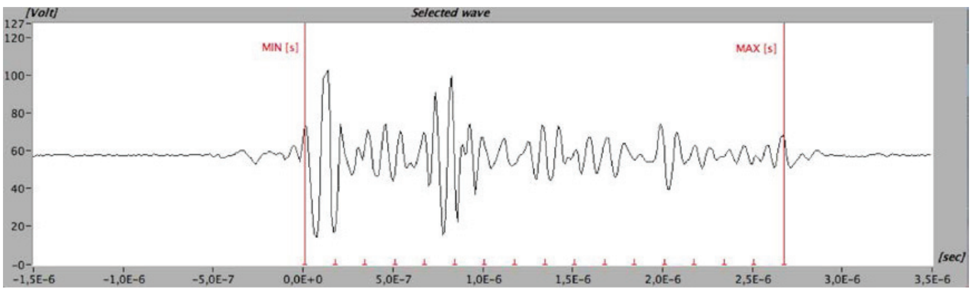

Fig. 4. Typical UT waveform of the UT volumetric file for the not impacted QHL3IM1 NCF composite laminate.

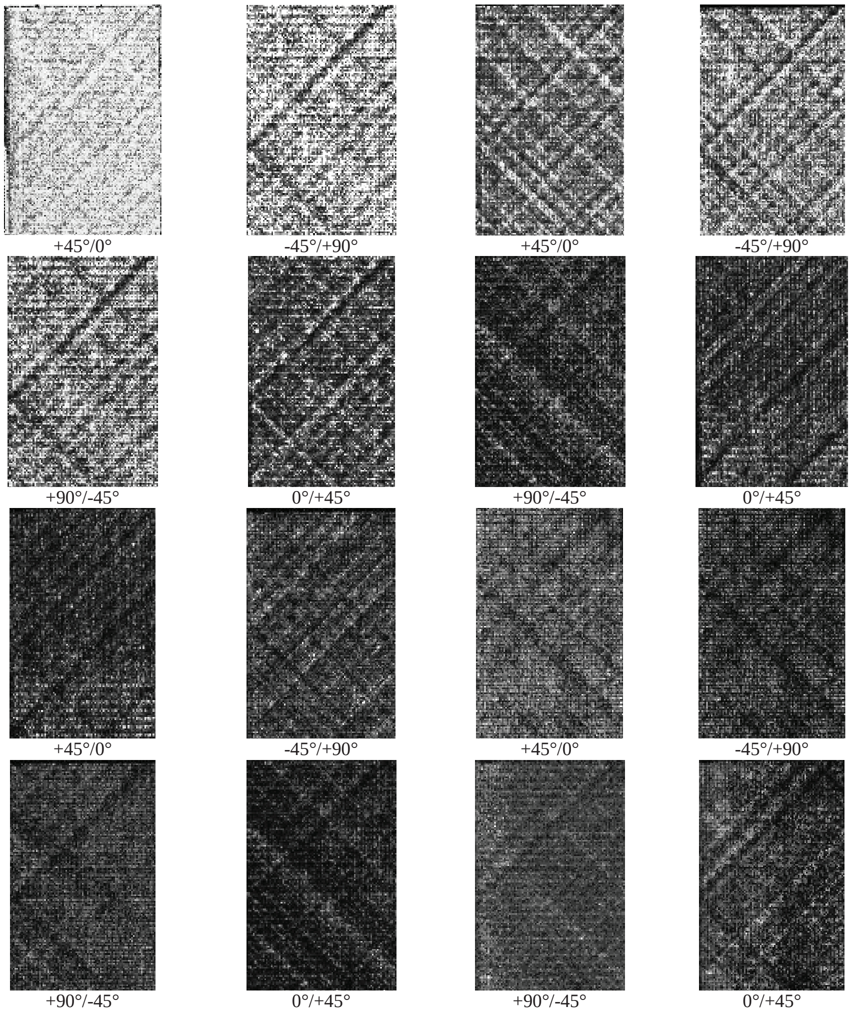

Fig. 5. Sixteen UT images of the not impacted quadriaxial laminate QHL3IM1. Each UT image, arranged in succession from left to right and from top to bottom, relates to 1/16 of the laminate nominal thickness comprising two diverse consecutive fiber orientations in the stacking sequence.

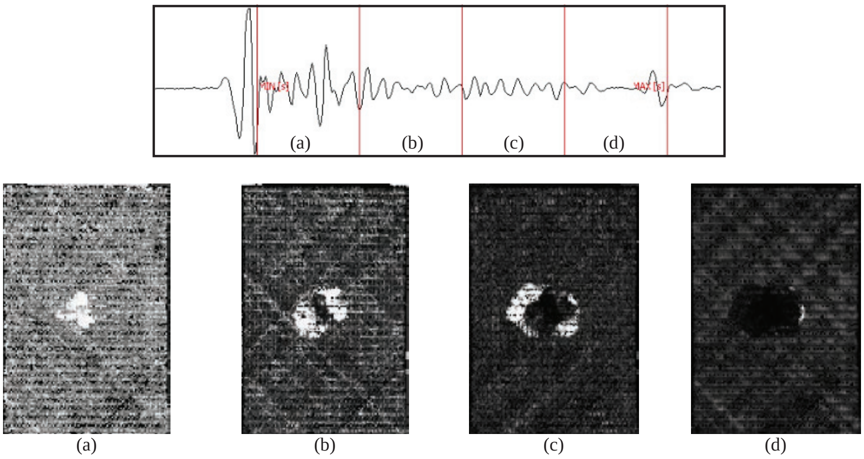

Fig. 6. Four UT images for low energy (9 J) impacted NCF laminate specimen QHL3IM2:
(a) surface damage, (b) and (c) internal damage, (d) in-plane projection of the total damage.

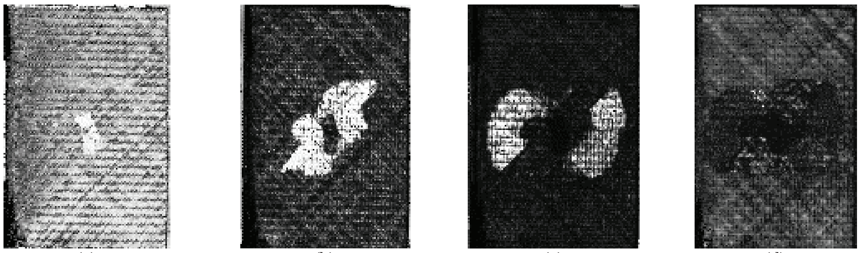

(a) (b) (c) (d)

Fig. 7. Four UT images for medium energy (20 J) impacted NCF laminate specimen QHL3IM5: (a) surface damage, (b) and (c) internal damage, (d) in-plane projection of the total damage.

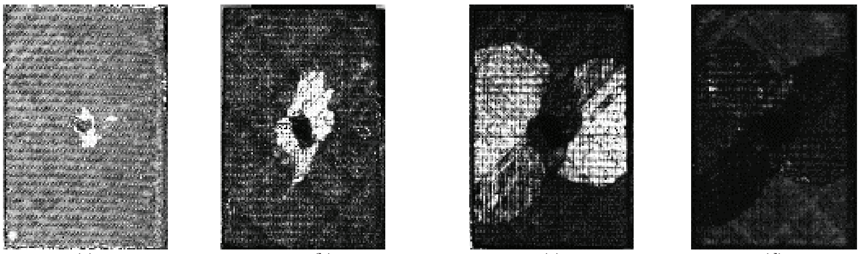

(a) (b) (c) (d)

Fig. 8. Four UT images for high energy (40 J) impacted NCF laminate specimen QHL3IM8: (a) surface damage, (b) and (c) internal damage, (d) in-plane projection of the total damage.

6. Conclusions

An advanced UT NDE procedure, based on complete UT waveform detection and analysis, was utilized to carry out the full volume (FV) UT immersion scanning of quadriaxial NCF composites subjected to impact loading conditions.

The main scope of the analysis was the metrological characterization of the NCF laminates in terms of actual thickness estimation and stacking sequence fiber orientation verification as well as the NCF composite quality assessment in terms of development and location of impact damage within the whole composite material volume.

The results showed that the FV-UT NDE technique is a very efficient tool for the metrological evaluation and damage characterization of impacted NCF composites.

The NCF laminate estimated thickness values were very close to the nominal values and the fiber orientations were found consistent with the designed stacking sequence.

The impact damage development was effectively characterized by evaluating the damage position in the laminate thickness direction and by identifying the different damage shapes at interfaces between layers with diverse fiber orientations in the stacking sequence.

Acknowledgements

This research work was carried out within Project “STEP FAR - Sviluppo di materiali e tecnologie ecocompatibili, di processi di foratura, taglio e di assemblaggio robotizzato” (PON03PE00129_1).

The Fraunhofer Joint Laboratory of Excellence for Advanced Production Technology at the Dept. of Chemical, Materials and Industrial Production Engineering, University of Naples Federico II, is gratefully acknowledged for its support to this work.

References

[1] Mallick PK. Fiber-reinforced composites: materials, manufacturing, and design, 3rd ed. CRC Press Taylor & Francis Group; 2007.

[2] Witik RA, Gailleb F, Teuscher R, Ringwald H, Michaud V. Economic and environmental assessment of alternative production methods for composite aircraft components. J Cleaner Production 2012; 29-30: 91-102

[3] Adden S, Horst P. Damage propagation in non-crimp fabrics under bi-axial static and fatigue loading. Comp Sci & Technol 2006; 66: 626-633.

[4] Mikhaluk DS, Truong TC, Borovkov AI, Lomov SV, Verpoest I. Experimental observations and finite element modelling of damage initiation and evolution in carbon/epoxy non-crimp fabric composites. Engineering Fracture Mechanics 2008; 75/9: 2751-2766.

[5] Bibo GA, Hogg PJ, Kemp M. Mechanical characterisation of glass and carbon fibre reinforced composites made with non-crimp fabrics. Comp Sci & Technol 1997; 57: 1221–41.

[6] Wang Y, Li J, Do BP. Properties of composite laminates reinforced with E-glass multiaxial non-crimp fabrics. J Comp Mat 1995; 29/17: 2317-33.

[7] Hashin Z. Analysis of cracked laminates: a variational approach, Mech Mater 1985; 4: 121-36.

[8] Talreja R. Internal variable damage mechanics of composite materials yielding, damage, and failure of anisotropic solids. In: Boehler JP. London: Mechanical Engineering Publications; 1990. p. 509-33.

[9] Edgren F, Mattsson D, Aspa LE,Varna J. Formation of damage and its effects on non-crimp fabric reinforced composites loaded in tension. Comp Sci & Technol 2004; 64 :675-692.

[10] Liu D, Malvern LE. Matrix cracking in impacted glass/epoxy plates, J Composite Materials 1987; 21: 594-609.

[11] Caprino G. Residual strength prediction of impacted CFRP laminates, J Comp Mat 1984; 18: 508-518.

[12] Hsu DK. Non-destructive evaluation (NDE) of aerospace composites: ultrasonic techniques. NDE of polymer matrix composites 2013, 397-422

[13] Teti R. Ultrasonic identification and measurement of defects in composite material laminates, CIRP Annals 1990, 39/1: 527-530.

[14] Thagard JR, Okoli OI, Liang Z, Wang HP, Zhang C. Resin infusion between double flexible tooling: prototype development. Composites Part A: Applied Science and Manufacturing 2003, 34/9: 803-811.

[15] Kessels JFA, Jonker AS, Akkerman R. Optimising the flow pipe arrangement for resin infusion under flexible tooling. Composites Part A: Applied Science and Manufacturing 2007; 38: 2076-2085.

[16] http://www.jleapt-unina.fraunhofer.it/

[17] Abrate S. Impact on composite structures, Cambridge Univ. Press; 1998